Damping Power System Electromechanical Oscillations Using Time Delays

Georgios Tzounas, *IEEE Student Member*, Rifat Sipahi, *IEEE Senior Member*, Federico Milano, *IEEE Fellow*

***Abstract*— This paper proposes to utilize intentional time delays as part of controllers to improve the damping of electromechanical oscillations of power systems. Through stability theory, the control parameter settings for which these delays in Power System Stabilizers (PSSs) improve the small signal stability of a power system are systematically identified, including the key parameter settings for which stability regions in the parameter plane remain connected for effective operation. The paper shows that PSSs with two control channels can be effectively designed to achieve best damping characteristics for a wide range of delays. Analytical results are presented on the One-Machine Infinite-Bus (OMIB) electromechanical power system model. To demonstrate the opportunities in more realistic dynamic models, our results are then implemented via numerical analysis on the IEEE standard 14-bus system.**

***Index Terms*— Small Signal Stability Analysis (SSSA), time-delayed control, Power System Stabilizer (PSS), power system control, delay-independent stability.**

I. Introduction

A. Motivation

Measurement and communication delays in local Power System Stabilizers (PSSs) and wide area damping controllers are a potential threat for the overall dynamic performance of power systems [1]–[3]. However, time delays are not always detrimental and can actually have unexpectedly beneficial effects on the stability of dynamical systems [4]–[8]. It has been shown, for example, that intentionally inserting a certain amount of delay in a feedback control system can enhance disturbance rejection capabilities, improve response time, and add the required damping to avoid undesired oscillations in a closed-loop system, see, e.g. [9]. More recently, analytical tuning techniques were proposed to engineer time delays and controller gains to achieve fast response [10]–[12]. These new results motivate the use of intentional time delays as part of controllers to effectively suppress poorly damped synchronous machine electromechanical oscillations.

B. Literature Review

Time delays appear in many control systems mainly because it takes time to measure/acquire information, formulate a decision based on this information, and implement the decision to achieve a particular control mission. Delays arise in many applications, such as in network control systems when sending/receiving information between physical locations [4], [13]; in connected vehicle models due to delays in communication/sensing lines and human reaction times [14], [15]; and in the dynamics of multi-agent systems [16], [17].

Since delays are in general a source of poor performance and instability, many studies have focused on the fundamentals of explaining these characteristics within a control theoretic approach [18]–[20]. Along these lines, stability theory has been developed to address the peculiarities of systems with delays and these results were more recently combined with powerful convex optimization tools to study the stability of and design controllers for time-delay systems, see, e.g. [21].

While most results in the literature treat delays as undesirable, there is also a large amount of work that has focused on the advantages of having delays in a closed-loop setting. In these studies, the goal is to incorporate delays intentionally into the closed-loop and systematically analyze the dynamics to show that for certain delays and controllers, the closed-loop dynamics can behave more desirably based on certain metrics, such as response time [9], [10], [22], [23]. A simple "delay-based" controller is the one in which a derivative of a signal $\dot{x}(t)$ is approximated using a first order Euler's approximation $\dot{x}(t) \approx (x(t) - x(t-\tau))/\tau$, where $\tau > 0$ is the delay [22].

Delay-based controllers have a rich history with many promising directions [5], [24], [25]. Recent studies have focused on analytical tractability. This is a challenging effort since delays cause infinite dimensional system dynamics, study of which cannot be performed using standard tools available for finite-dimensional systems. A remedy to this was proposed by utilizing some salient features of algebraic geometry on a class of delay systems, and deriving analytical formulae that prescribe how to tune the delays and control gains to achieve a desired performance from these systems [10]–[12]. These results have been recently extended to distributed control of multi-agent systems with the goal to achieve fast consensus of agents [26].

Despite the aforementioned advances, benefits of utilizing time delays as part of controllers are yet to be fully explored in engineering applications. In electric power engineering, the vast majority of studies have emphasized only the destabilizing effects of time delays [1]–[3]. Some studies have focused on modeling of delays that arise in wide area measurement systems [27], [28], while others have explored numerical methods for the stability analysis of power systems with inclusion of delays [29], [30]. Only very recently were delays

Georgios Tzounas and Federico Milano are with the School of Electrical and Electronic Engineering, University College Dublin, Ireland (e-mails: georgios.tzounas@ucdconnect.ie and federico.milano@ucd.ie).

Rifat Sipahi is with the Department of Mechanical and Industrial Engineering, Boston, MA (e-mail: r.sipahi@northeastern.edu).

This work is supported by the Science Foundation Ireland, by funding Georgios Tzounas and Federico Milano under Investigator Programme Grant No. SFI/15/IA/3074. A part of this manuscript was developed during G. Tzounas' visit at Northeastern University in Feb.-Mar. 2020.

in power systems viewed as tunable control design parameters [31], [32].

In light of the above discussion, there exists an opportunity to connect the recent results in time-delay systems literature toward improving the stability of power systems. The main goal of this paper is to systematically assess the impact of the structure and control parameter settings of delay-based PSSs on the small signal stability and in particular on the damping characteristics of power system electromechanical oscillations.

C. Contributions

The following are specific contributions of this paper:

- The One-Machine Infinite-bus (OMIB) system with inclusion of a Power System Stabilizer (PSS) is a relevant example of power system model that allows an analytical assessment of its stability when delays are considered. The paper shows the conditions for which the stability of the linearized OMIB equations is guaranteed independently from the magnitude of the delay, and present how system response time as measured by the concept of σ-stability can be understood in view of recent results [10].
- On the plane of controller gain vs intentional delay, the linearized equations of the OMIB system typically exhibit stable regions that are separated by unstable regions. This however does not allow tuning the "non-linear" dynamics to operate in separate stable regions as this would require the non-linear dynamics to first cross through an unstable region. The paper addresses this practically-relevant aspect of delayed dynamical systems by presenting the conditions under which the stable region of the OMIB system can be all "connected" so that the non-linear dynamics can be tuned for any settings inside this region.
- The paper extends, through numerical methods and the concept of ζ-stability, the analytical results based on the benchmark OMIB system to a more complex study. Specifically, the paper considers the IEEE standard 14-bus system model with the goal to achieve improved damping characteristics for a set of controller gains and intentional delays, and to achieve a fully connected stability region to be able to fully explore the parameter space, without introducing instability. The paper also examines the application of the proposed approach for the purpose of wide area damping control and discusses relevant practical aspects, such as the impact of communication delays with inclusion of noise and data packet dropouts.
- Finally, the paper demonstrates in what ways time delays can be utilized beneficially in power systems, adding to a large body of literature in which time delays were studied for their detrimental effects.

D. Organization

The remainder of the paper is organized as follows. Section II describes a comprehensive treatment for the stability analysis of small and large scale time-delay systems and provides the conditions for which the stability regions of a second-order Linear Time-Invariant (LTI) system in the delay vs control gain parameter space are all connected. Section III provides analytical results on the OMIB power system. Section IV discusses a case study based on the IEEE standard 14-bus system model. Finally, conclusions are drawn in Section V.

II. Spectral Analysis of Time-Delay Systems

This section first provides some preliminaries on the spectral properties of LTI systems with time delay. This is followed by further discussions on a second-order time-delay system. Then, for such system, the conditions that have to be satisfied to guarantee stability independently from the magnitude of the delay are deduced. Finally, it is shown how delay-independent stability enables "connected" stability regions.

A. Preliminaries

Since the study is concerned with the dynamics associated with small signals, it is relevant to provide below a concise discussion on the stability properties of linear systems affected by time delays. Given that the focus is on time-invariant systems, consider the following LTI system:

$$\dot{\boldsymbol{x}}(t) = \boldsymbol{A}_0\boldsymbol{x}(t) + \boldsymbol{A}_1\boldsymbol{x}(t-\tau), \tag{1}$$

where $\boldsymbol{A}_0$ and $\boldsymbol{A}_1$ are matrices with constant entries, delay is denoted by $\tau \geq 0$, and $\boldsymbol{x}$, $\boldsymbol{x} \in \mathbb{R}^n$, is the state vector. System (1) is a set of functional differential equations known as Delay Differential Equations (DDEs). Moreover, this system is of retarded type, i.e. the highest derivative of the state is not influenced by the delay term.

To assess exponential stability of system (1), one must study its characteristic roots, which are the zeros of the system characteristic function given by:

$$f(s,\tau) = \det\left|s\boldsymbol{I}_n - \boldsymbol{A}_0 - \boldsymbol{A}_1 e^{-\tau s}\right|, \tag{2}$$

where s denotes the complex Laplace variable, $\boldsymbol{I}_n$ is the identity matrix of dimensions $n \times n$, and the delay appears in the exponents as per Laplace transform. Due to the presence of the exponential function, this equation is not in polynomial form in s; it is instead called a quasi-polynomial in the literature [33].

Then one has that, for a given delay τ, system (1) is exponentially stable if and only if all its characteristic roots s^* have negative real parts. That is, for all s^* satisfying $f(s^*,\tau) = 0$, $\Re(s^*) < 0$ holds [7]. While in principle the stability definition is not different from that for ordinary differential equations[1], computing s^* to assess stability is challenging due to the transcendental exponential terms in $f(s,\tau)$ that arise due to the delay τ. This is because these terms bring about infinitely many characteristic roots, computation of which is prohibitive [4].

A remedy to the above issue is to recognize that the characteristic roots of the system vary on the complex plane in a continuum as the delay parameter changes in a continuum [34]. Hence, the only way the system may become unstable is that a characteristic root (or a pair of roots) touches the imaginary axis of the complex plane at $s = jw$, $w \in \mathbb{R}^+$.

[1]This is mainly because the spectrum of 'retarded' type LTI systems exhibit similar characteristics as those of ordinary differential equations [7].

That is, whenever $f(jw,\tau)=0$ for some $w\geq 0$ and τ, the system "may be" in transition from stability to instability, or vice versa[2].

Definition 1. Consider that $s^*_{i,i+1}=\alpha_i\pm j\beta_i$ define a pair of roots of (2). Then, the system is called:

- σ-stable, if $\forall\, i\in\mathbb{N}^*$, $\alpha_i<-\sigma$, where $\sigma>0$ is a prescribed exponential decay rate [10].
- ζ-stable, if $\forall\, i\in\mathbb{N}^*$, $\frac{-\alpha}{\sqrt{\alpha^2+\beta^2}}<\zeta$, where ζ is a prescribed dominant oscillation damping ratio.

Since (2) has infinitely many roots, here $\mathbb{N}^*$ denotes all natural numbers except for zero.

B. Analytical Study of Second-Order LTI Systems

This section starts with some salient stability characteristics of second-order LTI systems [11], [35], namely, a subset of the systems described by equation (1). It next demonstrates the parametric conditions for delay-independent stability and utilizes this information to characterize the connectedness of the arising stability regions in the parameter space.

1) System description: Consider the LTI system:

$$\ddot{x}(t)+c_1\dot{x}(t)+c_2x(t)=-u(t)\,, \tag{3}$$

where $c_1,c_2,\in\mathbb{R}$ and $u(t)$ is a scalar input. Next, let $u(t)$ be defined as a delay-based controller. Specifically, u is designed as Proportional Retarded (PR) controller:

$$u(t)=k_pz(t)-k_rz(t-\tau_r)\,, \tag{4}$$

where k_p and k_r, are the proportional and retarded gains, respectively; $\tau_r\geq 0$ is a constant delay; and $z(t)$ is the control input signal. This paper considers that $z(t)=\dot{x}(t)$, since this is the case that is of interest in power system applications (see the example discussed in Section III). Substitution of $z(t)=\dot{x}(t)$ in (5) yields:

$$u(t)=k_p\dot{x}(t)-k_r\dot{x}(t-\tau_r)\,. \tag{5}$$

The delay τ_r is intentional and hence its value can be effectively designed to be constant, as is the case with the controlled parameters of any device. Combining (3) and (5), and taking the Laplace transform of the arising dynamics leads to the closed-loop system characteristic equation $q(s,\tau_r,k_r)=0$, where

$$q(s,\tau_r,k_r)=s^2+(c_1+k_p)s+c_2-k_rse^{-s\tau_r}\,, \tag{6}$$

is the system characteristic equation.

2) σ-stability analysis : In order to study the σ-stability of system (3), the change of variable $s\rightarrow(s-\sigma)$ is applied to (6). This yields the following quasi-polynomial:

$$\tilde{q}(\sigma,s,\tau_r,k_r)=\tilde{q}_0(\sigma,s)+\tilde{q}_1(\sigma,s)k_re^{\sigma\tau_r}e^{-s\tau_r}\,, \tag{7}$$

where

$$\begin{aligned}\tilde{q}_0(\sigma,s)&=(s-\sigma)^2+(c_1+k_p)(s-\sigma)+c_2\,,\\ \tilde{q}_1(\sigma,s)&=-(s-\sigma)\,.\end{aligned}$$

[2]Note that it is necessary, but not sufficient, that the system has at least one root on the imaginary axis for its transition from stable to unstable behavior. For sufficiency, the system must be stable for $\tau-|\varepsilon|$, $|\varepsilon|\ll 1$.

Recall that the roots of the characteristic equation change continuously with respect to variations of system parameters and time delays. That said, the system may change from stable to unstable, and vice versa, only if a root (or a pair of roots) crosses the imaginary axis of the complex plane.

Hence, the σ-stability of (3) can be assessed by finding the set of crossing points $(\tau_r^{\rm cr},k_r^{\rm cr})$, that satisfy:

$$\tilde{q}(\sigma,jw,\tau_r^{\rm cr},k_r^{\rm cr})=0\,, \tag{8}$$

where s has been substituted for jw. The set $(\tau_r^{\rm cr},k_r^{\rm cr})$ can be determined by considering the magnitude and the argument of (8), as follows [11], [35]:

$$\begin{aligned}\tau_r^{\rm cr}=\frac{1}{jw}\Big(&\mathrm{Arg}(\tilde{q}_1(\sigma,jw))-\mathrm{Arg}(\tilde{q}_0(\sigma,jw))\\&+\frac{\pi}{2}(4\mu+\nu+1)\Big)\,,\end{aligned} \tag{9}$$

$$k_r^{\rm cr}=\nu e^{-\sigma\tau_r^{\rm cr}}\left|\frac{\tilde{q}_0(\sigma,jw)}{\tilde{q}_1(\sigma,jw)}\right|\,, \tag{10}$$

where $\nu=\pm1$, $\mu\in\mathbb{Z}$. Since $\mu\in\mathbb{Z}$, there exist infinitely many crossing points $(\tau_r^{\rm cr},k_r^{\rm cr})$ that satisfy (9) and (10) which show up periodically. Moreover, since $\nu=\pm1$ in (10) crossing points appear for both positive and negative gains. Furthermore, by employing (9) and (10), one can trace the domains of stability that correspond to specified exponential decay rates, i.e. the *σ-stability map* in the (τ_r,k_r) space.

Finally, note that if the time-delayed state in (3) is not utilized, i.e. $k_r=0$, then the closed-loop system behavior is determined by the polynomial $\tilde{q}_0(\sigma,s)$. In this case, dissipative terms included in the system are defined by the coefficient of s corresponding to the first derivative of the state:

$$c=c_1+k_p\,. \tag{11}$$

Here, the coefficient c_1 defines the damping of the open-loop system oscillatory mode, while k_p defines the amount of non-delayed artificial damping introduced by the PR controller.

3) Delay-independent stability: $\mathcal{K}\subset\mathbb{R}$, such that the dynamics are stable regardless of the magnitude of the time delay τ_r.

For a given set $\mathcal{K}$, a necessary condition for delay independent stability is that the roots of the system characteristic equation never cross the imaginary axis, or equivalently:

$$q(jw,\tau_r,k_r)\neq 0\ ,\ \forall\tau_r\geq 0,\ \forall k_r\in\mathcal{K}\,. \tag{12}$$

Condition (12) is also sufficient, provided that, with $\tau_r=0$ and an arbitrary gain in $\mathcal{K}$, the roots of the characteristic equation have negative real parts.

Using (11) in (12) yields[3]:

$$\begin{aligned}&-w^2+cjw+c_2-k_rjwe^{-jw\tau_r}\neq 0\\ \Rightarrow\quad&\frac{-w^2+cjw+c_2}{k_rjw}\neq e^{-jw\tau_r}\\ \Rightarrow\quad&\frac{c}{k_r}+j\frac{1}{k_r}(w-\frac{c_2}{w})\neq e^{-jw\tau_r}\,,w\neq 0\,.\end{aligned} \tag{13}$$

[3]Clearly, for $c_2\neq 0$, $w=0$ is not a solution. Hence, only the case of $w\neq 0$ is investigated.

Notice that the real part of (13) does not depend on w, and thus, in the complex plane, the left hand side defines the vertical line with abscissa c/k_r. In addition, $e^{-jw\tau_r}$ defines in the complex plane a unit circle centred at $(0,0)$, regardless of the value of the delay τ_r. That said, the critical condition for delay independent stability is that the line c/k_r is tangent to the unit circle. Equivalently, one has:

$$c = \pm k_r \,. \tag{14}$$

Remark 1. *(Connectedness of stability regions).* The following cases are deduced from (14):

- If $c = -k_r^0 < 0$, $k_r = k_r^0 > 0$, the system is delay independent unstable in $\mathcal{K} = (-k_r^0, k_r^0)$. Since $c < 0$, the system is unstable around the origin of the τ_r-k_r plane. Hence, even if stable regions exist, these regions are guaranteed to be disconnected.
- If $c = 0$, there are no delay independent stable or unstable regions.
- If $c = k_r^0 > 0$, $k_r = k_r^0 > 0$, the system is delay independent stable in $\mathcal{K} = (-k_r^0, k_r^0)$. The existence of a delay independent stable region around the zero gain guarantees that there is a large connected stable domain in the τ_r-k_r plane. This feature is very important for two reasons: *(i)* there is the possibility that the dynamics can be characterized by favorable σ- and ζ-stability properties for large delay values, *(ii)* the presence of a delay-independent stable region indicates that there exists at least one large, "connected" stable region from zero to infinite delay.

Notice that the delay independent stable/unstable region is symmetric with respect to the gain k_r.

C. Linear Large-Scale Time-Delay Systems

For a second-order LTI system with PR control, such as the one discussed above, one can analytically identify the parameter regions with specified exponential decay rates, as well as the conditions for delay independent stability. However, real-world dynamical systems are larger in size and much more complex. Capturing the impact of delays on the behavior of large system models can be achieved only by carrying out a numerical analysis. Nevertheless, these studies must be carefully guided by our analytical understanding of small scale dynamical systems. This is the approach we aim to take in what follows.

We describe next how to assess the stability of large scale linear time-delay systems. To this aim, system (1) is extended to include multiple delays τ_i. The resulting LTI dynamical system is described through the following set of DDEs:

$$\dot{\boldsymbol{x}}(t) = \boldsymbol{A}_0\boldsymbol{x}(t) + \sum_{i=1}^{\rho} \boldsymbol{A}_i\boldsymbol{x}(t-\tau_i)\,, \tag{15}$$

where $\tau_i \geq 0$, $i = 1, 2, \ldots, \rho$, The characteristic matrix of (15) has the following form [29]:

$$s\boldsymbol{I}_n - \boldsymbol{A}_0 - \sum_{i=1}^{\rho} \boldsymbol{A}_i e^{-s\tau_i}\,. \tag{16}$$

Since (16) is transcendental, it has infinitely many eigenvalues, and only an approximation of the solution is possible. Different approaches have been proposed to overcome this problem [29]. In this paper, the DDE system (15) is transformed to a formally equivalent set of Partial Differential Equations (PDEs), which has infinite dimensions. The PDE system is then reduced to a finite dimensional problem through Chebyshev spectral discretization [36], [37]. If N_C is the number of points of the Chebyshev differentiation matrix [29], then discretization leads to an approximate linear matrix pencil in the form:

$$s\boldsymbol{I}_{nN_C} - \boldsymbol{M}\,, \tag{17}$$

where the matrix $\boldsymbol{M}$ has dimensions $nN_C \times nN_C$. The spectrum of (17) – which can be found using any common numerical technique, e.g. the QR method – represents an approximate spectrum of (16). The Chebyshev spectral discretization technique has been successfully applied to single and multiple time-delay systems, e.g. to power systems with constant and stochastic delays affecting damping controllers [28], [38].

After the above analysis is complete, one can reveal the most critical eigenvalue(s), by comparing the damping ratios ζ_i of all computed eigenvalues. This work focuses on the parametric analysis in a delay vs control gain space. The above analysis allows building a map of specified dominant oscillation damping ratio ζ. In the remainder of the paper, this map is referred to as the *ζ-stability map*.

D. Non-linear Large-Scale Time-Delay Systems

Real-world dynamical systems, such as, for example, high-voltage transmission systems, are conventionally described through a set of non-linear Differential-Algebraic Equations (DAEs), as follows:

$$\begin{aligned} \dot{\boldsymbol{x}} &= \boldsymbol{f}(\boldsymbol{x}, \boldsymbol{y})\,, \\ \boldsymbol{0}_{m,1} &= \boldsymbol{g}(\boldsymbol{x}, \boldsymbol{y})\,, \end{aligned} \tag{18}$$

where $\boldsymbol{f}$ ($\boldsymbol{f} : \mathbb{R}^{n+m} \to \mathbb{R}^n$), $\boldsymbol{g}$ ($\boldsymbol{g} : \mathbb{R}^{n+m} \to \mathbb{R}^m$) are the differential and algebraic equations; $\boldsymbol{x}$, $\boldsymbol{x} \in \mathbb{R}^n$, and $\boldsymbol{y}$, $\boldsymbol{y} \in \mathbb{R}^m$, are the state and algebraic variables, respectively; and $\boldsymbol{0}_{m,1}$ denotes the $m \times 1$ zero matrix. For simplicity, the time dependency has been omitted from (18).

The presence of time delays, for example, in control loops, changes the set of DAEs (18) into a set of Delay Differential Algebraic Equations (DDAEs). A non-linear dynamical system with inclusion of delays can be described as:

$$\begin{aligned} \dot{\boldsymbol{x}} &= \boldsymbol{f}(\boldsymbol{x}, \boldsymbol{y}, \boldsymbol{x}_d, \boldsymbol{y}_d)\,, \\ \boldsymbol{0}_{m,1} &= \boldsymbol{g}(\boldsymbol{x}, \boldsymbol{y}, \boldsymbol{x}_d, \boldsymbol{y}_d)\,, \end{aligned} \tag{19}$$

where $\boldsymbol{x}_d$, $\boldsymbol{x}_d \in \mathbb{R}^{n_d}$, and $\boldsymbol{y}_d$, $\boldsymbol{y}_d \in \mathbb{R}^{m_d}$ are the delayed state and algebraic variables, respectively. Suppose that the system includes a single constant delay τ. Then, one has:

$$\begin{aligned} \boldsymbol{x}_d &= \boldsymbol{x}(t-\tau)\,, \\ \boldsymbol{y}_d &= \boldsymbol{y}(t-\tau)\,, \end{aligned} \tag{20}$$

where t is the current time. When $\boldsymbol{y}_d$ does not appear in the algebraic equations of (19), this leads to the index-1

Hessenberg form of DDAEs:

$$\begin{aligned} \dot{\boldsymbol{x}} &= \boldsymbol{f}(\boldsymbol{x}, \boldsymbol{y}, \boldsymbol{x}_d, \boldsymbol{y}_d)\,, \\ \boldsymbol{0}_{m,1} &= \boldsymbol{g}(\boldsymbol{x}, \boldsymbol{y}, \boldsymbol{x}_d)\,. \end{aligned} \tag{21}$$

Model (21) is adopted instead of (19), since it allows simplifying the form of the characteristic equation of the corresponding linearized system, while being adequate for the applications considered in this paper. The interested reader can find a detailed study on the Small Signal Stability Analysis (SSSA) for non-index 1 Hessenberg form systems of DDAEs in [39].

For sufficiently small disturbances, and for the purpose of SSSA, (21) can be linearized around a valid stationary point, as follows:

$$\Delta\dot{\boldsymbol{x}} = \boldsymbol{f}_{\boldsymbol{x}}\Delta\boldsymbol{x} + \boldsymbol{f}_{\boldsymbol{y}}\Delta\boldsymbol{y} + \boldsymbol{f}_{\boldsymbol{x}_d}\Delta\boldsymbol{x}_d + \boldsymbol{f}_{\boldsymbol{y}_d}\Delta\boldsymbol{y}_d\,, \tag{22}$$

$$\boldsymbol{0}_{m,1} = \boldsymbol{g}_{\boldsymbol{x}}\Delta\boldsymbol{x} + \boldsymbol{g}_{\boldsymbol{y}}\Delta\boldsymbol{y} + \boldsymbol{g}_{\boldsymbol{x}_d}\Delta\boldsymbol{x}_d\,, \tag{23}$$

where $\boldsymbol{f}_{\boldsymbol{x}}$, $\boldsymbol{f}_{\boldsymbol{y}}$, $\boldsymbol{g}_{\boldsymbol{x}}$, $\boldsymbol{g}_{\boldsymbol{y}}$, are the Jacobian matrices of the delay-free variables; and $\boldsymbol{f}_{\boldsymbol{x}_d}$, $\boldsymbol{f}_{\boldsymbol{y}_d}$, $\boldsymbol{g}_{\boldsymbol{x}_d}$, are the Jacobian matrices of the delayed variables of (22) and (23).

In the linearized system (22), (23), the algebraic variables $\Delta\boldsymbol{y}$, $\Delta\boldsymbol{y}_d$ can be eliminated, under the assumption that $\boldsymbol{g}_{\boldsymbol{y}}$ is not singular. Substitution of (23) into (22) yields:

$$\Delta\dot{\boldsymbol{x}}(t) = \boldsymbol{A}_0\Delta\boldsymbol{x}(t) + \boldsymbol{A}_1\Delta\boldsymbol{x}(t-\tau) + \boldsymbol{A}_2\Delta\boldsymbol{x}(t-2\tau)\,, \tag{24}$$

where

$$\begin{aligned} \boldsymbol{A}_0 &= \boldsymbol{f}_{\boldsymbol{x}} - \boldsymbol{f}_{\boldsymbol{y}}{\boldsymbol{g}_{\boldsymbol{y}}}^{-1}\boldsymbol{g}_{\boldsymbol{x}}\,, \\ \boldsymbol{A}_1 &= \boldsymbol{f}_{\boldsymbol{x}_d} - \boldsymbol{f}_{\boldsymbol{y}}{\boldsymbol{g}_{\boldsymbol{y}}}^{-1}\boldsymbol{g}_{\boldsymbol{x}_d} - \boldsymbol{f}_{\boldsymbol{y}_d}\boldsymbol{g}_{y}^{-1}\boldsymbol{g}_{\boldsymbol{x}}\,, \\ \boldsymbol{A}_2 &= -\boldsymbol{f}_{\boldsymbol{y}_d}\boldsymbol{g}_{y}^{-1}\boldsymbol{g}_{\boldsymbol{x}_d}\,. \end{aligned}$$

Applying the Laplace transform in (24) yields the following, quasi-polynomial characteristic matrix:

$$s\boldsymbol{I}_n - \boldsymbol{A}_0 - \boldsymbol{A}_1 e^{-s\tau} - \boldsymbol{A}_2 e^{-2s\tau}\,. \tag{25}$$

Note that the form of the characteristic matrix (25) can be retrieved from (16) for $\rho = 2$ and $\tau_2 = 2\tau_1$.

III. One-Machine Infinite-Bus System

The OMIB system shown in Fig. 1 serves well for illustration purposes since it is the simplest power system dynamic model and is analytically tractable. This section first describes the classical machine model and then includes in this model a simplified PSS with a Proportional-Retarded (PR) control, i.e. with two input signals, one instantaneous and one delayed. The results presented in Section II-B are critical to establish the stability features of the closed-loop system.

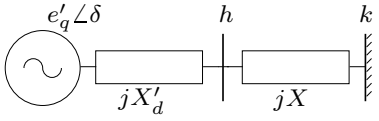

Fig. 1. Single-line diagram of the OMIB system.

A. Classical Model

The classical per-unit model of this system is as follows [40]:

$$\begin{aligned} \dot{\delta} &= \Omega_b(\omega - \omega_o)\,, \\ 2H\dot{\omega} &= p_m - p_e(\delta) - D(\omega - \omega_o)\,, \end{aligned} \tag{26}$$

where δ, ω, are the rotor angle and the rotor speed of the synchronous machine, respectively; p_m and p_e are the mechanical, electrical power output of the machine, respectively. In addition, H is the machine inertia constant; D is the machine rotor damping coefficient; ω_o is the system reference angular speed; and Ω_b is the nominal synchronous angular frequency in rad/s. The time dependency has been omitted from (26) for simplicity.

The electrical power p_e is described by the following nonlinear expression:

$$p_e(\delta) = \frac{e'_q v_k}{X_{\text{tot}}}\sin(\delta - \theta_k)\,, \tag{27}$$

where v_k, θ_k, are the (constant) voltage magnitude and angle at the infinite bus k; e'_q is the internal electromotive force of the synchronous machine, which is taken as constant, by assuming an integral Automatic Voltage Regulator (AVR). X_{tot} is the total reactance, comprising the machine transient reactance (X'_d) and the line reactance (X), where the latter is referred to the machine power base.

Defining the system state vector as $[\delta \;\; \omega]^T$, making use of (27) and linearizing (26) around a valid equilibrium $[\,\delta_o \;\; \omega_o\,]^T$ yield:

$$\Delta\dot{\delta} = \Omega_b\Delta\omega\,, \tag{28}$$

$$2H\Delta\dot{\omega} = -\frac{e'_q v_k \cos(\delta_o - \theta_k)}{X_{\text{tot}}}\Delta\delta - D\Delta\omega\,, \tag{29}$$

where $\Delta\delta = \delta - \delta_o$ and $\Delta\omega = \omega - \omega_o$. Equations (28)-(29) can be rewritten as a second-order LTI system:

$$\Delta\ddot{\delta} + d\Delta\dot{\delta} + b\Delta\delta = 0\,, \tag{30}$$

where $\Delta\delta \equiv x$ and

$$b = \frac{\Omega_b e'_q v_k \cos(\delta_o)}{2HX_{\text{tot}}}, \qquad d = \frac{D}{2H}\,. \tag{31}$$

B. Power System Stabilizer with PR Control

In power systems, measurements of synchronous machine rotor speeds are available in practice, whereas measurements of rotor angles are not. Thus, in its simplest form, the PSS measures the machine rotor speed variation, i.e. $\Omega_b^{-1}\Delta\dot{\delta} = \Delta\omega$, and introduces a fictitious damping into the swing equation (29). The linearized closed-loop system can therefore be written as:

$$\Delta\ddot{\delta} + d\Delta\dot{\delta} + b\Delta\delta = -u(\Delta\dot{\delta})\,. \tag{32}$$

The damping controller is modeled here as a proportional PSS with two control channels, one with and one without delay. The PSS diagram is shown in Fig. 2.

Dual-channel PSSs have been employed in the past, e.g. as decentralized-hierarchical schemes for wide-area stabilizing control [41]. The dual-channel PSS output is described as:

$$u = k_p\Delta\dot{\delta} - k_r\Delta\dot{\delta}(t - \tau_r)\,. \tag{33}$$

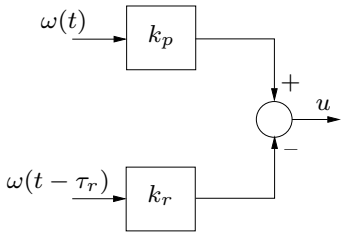

Fig. 2. PR control-based PSS diagram.

Merging (28), (32) and (33) leads to the following closed-loop system representation:

$$\Delta\ddot{\delta} + (d + \frac{k_p}{\Omega_b})\Delta\dot{\delta} + b\Delta\delta - \frac{k_r}{\Omega_b}\Delta\dot{\delta}(t-\tau_r) = 0\,. \qquad (34)$$

which is exactly in the form of (3)-(5). Applying the Laplace transform and substituting the initial conditions $\Delta\delta(0) = \Delta\dot{\delta}(0) = 0$, yields the following characteristic quasi-polynomial:

$$q(s,\tau_r,k_r) = s^2 + (d + \frac{k_p}{\Omega_b})s + b - \frac{k_r}{\Omega_b}se^{-s\tau_r}\,. \qquad (35)$$

Comparing the quasi-polynomial (35) with the one in (6), one has $c_1 = d$, $c_2 = b$, $= \Omega_b^{-1}$. Therefore, the analysis of σ-stability and the conditions for delay independent stability can be studied through the derivations of Section II-B. The amount of friction included in the delay-free OMIB system is according to (11):

$$c = d + \frac{k_p}{\Omega_b}\,. \qquad (36)$$

The critical condition for which the OMIB system is delay independent stable is that $\Omega_b c/k_r$ is tangent to the unit circle. Equivalently, one has:

$$c = \pm\frac{k_r}{\Omega_b}\,. \qquad (37)$$

C. Illustrative example

This section provides a numerical example on the closed-loop OMIB system. Let $e'_q = 1.22$ pu, $v_k = 1$ pu, $\theta_k = 0$ rad, $p_m = 1$ pu, $X_{\rm tot} = 0.7$ pu. The initial value δ_o of the rotor angle is given by:

$$\delta_o = \arcsin\left(\frac{p_m X_{\rm tot}}{v_k e'_q}\right)\,. \qquad (38)$$

The examined equilibrium is hence $[0.61\,,\,1]^T$. Let also $H = 2.5$ MWs/MVA, and $\Omega_b = 100\pi$ rad/s (50 Hz system). Then, $b = 89.756$ pu in (30). The cases below construct the σ-stability map of the system for the three cases of negative, zero and positive values of c at this fixed equilibrium.

Case 1: For $c = -0.4 < 0$, the stability map is shown in Fig. 3. The map has a symmetric delay independent unstable region obtained for $k_r \in (-125.6, 125.6)$. In addition, PR control can stabilize the system, provided that the delay is $\tau_r < 0.131$ s and a proper $k_r > 0$ is selected (see e.g. point $P_1(0.05, 729)$). The maximum value of σ in the visible part of the map shown in Fig. 3 is 4.32.

Stable regions of the map in Fig. 3 also exist for delays higher than 0.131 s. For example, the system is stable around the point $P_3(0.30, -763.4)$. Note, however, that obtaining the equilibrium of a delayed system implies that a time equal to the maximum delay included in the system has elapsed but, meanwhile, the system may have been already rendered unstable. Indeed, Fig. 3 indicates that there is no path to P_3 without crossing the system stability boundary, which implies that the system necessarily becomes unstable before actually reaching P_3. A relevant consequence is that in this case there is no way to operate the system in a stable equilibrium for negative gain values.

It is relevant to illustrate the effect of crossing the stability boundary of the closed-loop OMIB system by carrying out a time domain simulation. Suppose that the non-linear system (26) with the inclusion of the PR controller (33), operates around the stable equilibrium defined by the point P_1 of Fig. 3.

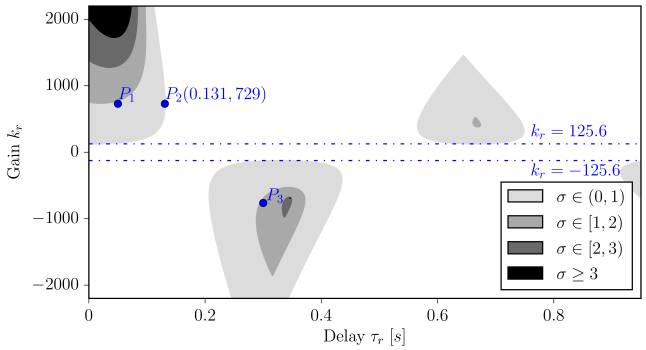

Fig. 3. Closed-loop linearized OMIB system: σ-stability map in the τ_r-k_r plane, $c = -0.4$.

The system is numerically integrated considering a small noise on the measurement of the OMIB rotor speed. The noise is a normal process with zero mean and standard deviation of 0.0002. The noise amplitude is set to a small value with the purpose of showing the dynamics of the system in a neighbourhood of the equilibrium point. At $t = 2$ s, the gain and delay are switched to $k_r = -765$ and $\tau_r = 0.3$, respectively, so that the system is set at the new equilibrium point P_3.

Fig. 4 shows the simulation result, and indicates that, as expected, attempting to jump to a different, not connected stable region by crossing the stability boundary during a transient, renders the system unstable. Thus, P_3 is an example of an infeasible stationary point, and thus, the delay margin of the system is 0.131 s.

Case 2: The σ-stability map for $c = 0$ is presented in Fig. 5. In this case, the stability of the system depends on the magnitude of the delay, regardless of the value of the gain k_r. In fact, the horizontal line $k_r = 0$ comprises bifurcation points. The delay-free closed-loop system is stable for $k_r > 0$ and unstable for $k_r < 0$. Provided that a proper positive k_r value is selected and that $\tau_r < 0.166$ s (see point P_4), the delayed system is stable. For completeness, we mention that the maximum value of σ in the visible part of Fig. 5 is 4.68.

There also exist stable regions for $\tau_r > 0.166$ s. For example, the system is small-signal stable around P_5. However,

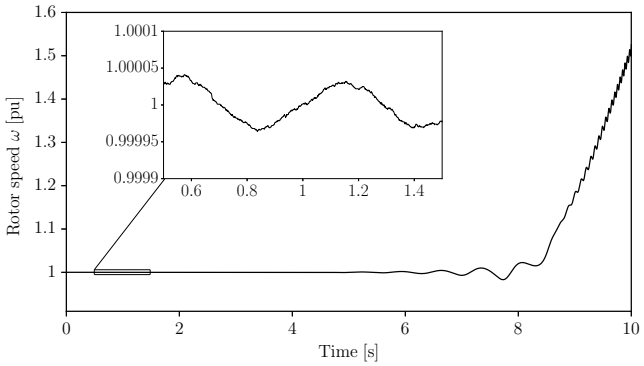

Fig. 4. Closed-loop non-linear OMIB system (26) with noisy rotor speed measurement: the equilibrium is switched from P_1 to P_3 at $t = 2$ s.

similarly to the discussion of *Case 1*, the system destabilizes before actually reaching P_5. The reason for this is that one must go through the point P_4 while staying inside the stable regions, however this point is bifurcation point and is technically unstable due to having $\sigma = 0$, or equivalently zero damping.

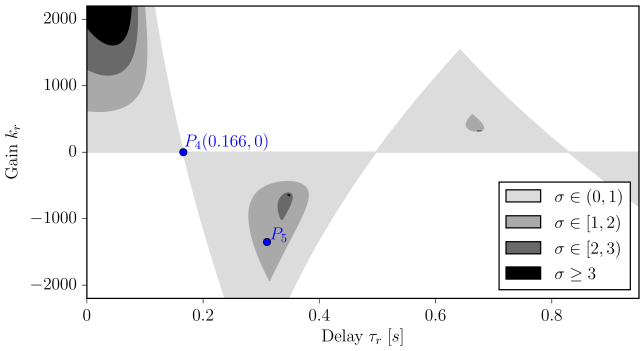

Fig. 5. Closed-loop linearized OMIB system: σ-stability map in the τ_r-k_r plane, $c = 0$.

Case 3: The stability map for $c = 0.4 > 0$ is shown in Fig. 6. In this case, the stable region is compact. For $k_r \in (-125.6, 125.6)$ the system is stable regardless of the magnitude of the delay τ_r. Moreover, all points of Fig. 6 with $\sigma > 0$ represent stable and feasible stationary points of the linearized OMIB system. For example, such points are $P_6(0.13, 400)$ and $P_7(0.35, -410)$. The maximum value of σ in the map as presented in Fig. 6 is 5.07.

A time domain simulation is carried out including the same noise model on the rotor speed measurement as in *Case 1*. At $t = 2$ s, the system equilibrium is switched from P_6 to P_7. The resulting plot, presented in Fig. 7, shows that the machine maintains synchronism.

Overall, proper design of the PSS given by the PR law (33) allows unifying the σ-stable regions, and thus allows one to operate the OMIB system under the presence of large delays. In particular, this is achieved by properly adjusting the control parameter k_p which introduces delay-free artificial damping to the system.

Finally, the delay τ_r in this example is assumed to be a fully controlled parameter. However, the above discussion is

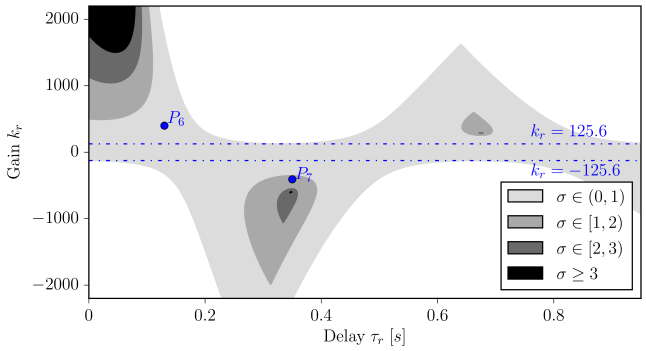

Fig. 6. Closed-loop linearized OMIB system: σ-stability map in the τ_r-k_r plane, $c = 0.4$.

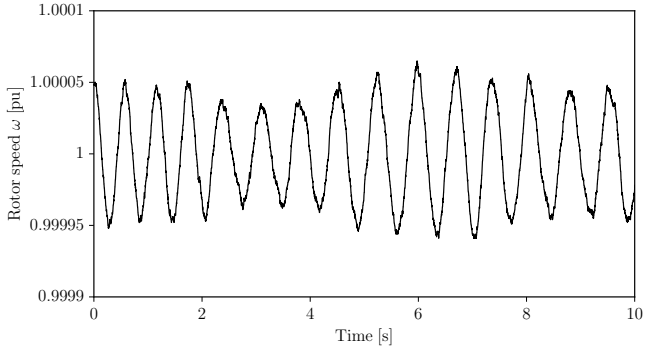

Fig. 7. Closed-loop non-linear OMIB system (26) with noisy rotor speed measurement: at $t = 2$ s, the equilibrium is switched from P_6 to P_7 shown in Fig. 6.

relevant also for systems with inherent delays. For the sake of example, consider again point P_6 of Fig. 6. Suppose that the corresponding delay, i.e. 0.13 s, represents an uncontrolled physical phenomenon, e.g. the latency of a measurement transmitted through a communication system. In power systems, this situation describes, for example, the behavior of a Wide Area Measurement System (WAMS) [28]. In such a scenario, the parameter τ_r can be adaptively adjusted to add an artificial delay, which ensures that the system under the total delay $0.13 + \tau_r$ always operates at a region of high exponential decay rate. Along these lines, see, for example, the idea of delay scheduling in [9].

IV. Case Study

This case study discusses the stability characteristics of the IEEE 14-bus system depicted in Fig. 8. The system consists of fourteen buses, five synchronous machines, twelve loads, twelve transmission lines and four transformers. All machines are equipped with Automatic Voltage Regulators (AVRs). The static and dynamic data of the system can be found in [42]. Simulations in this section are carried out using the Python-based power system analysis software tool Dome [43].

Without any PSS installed to the system, SSSA shows that the rightmost pair of eigenvalues is $0.3522 \pm j9.12$, and thus, the system is unstable around the examined equilibrium. This situation can be fixed through a PSS. The PSS employed in

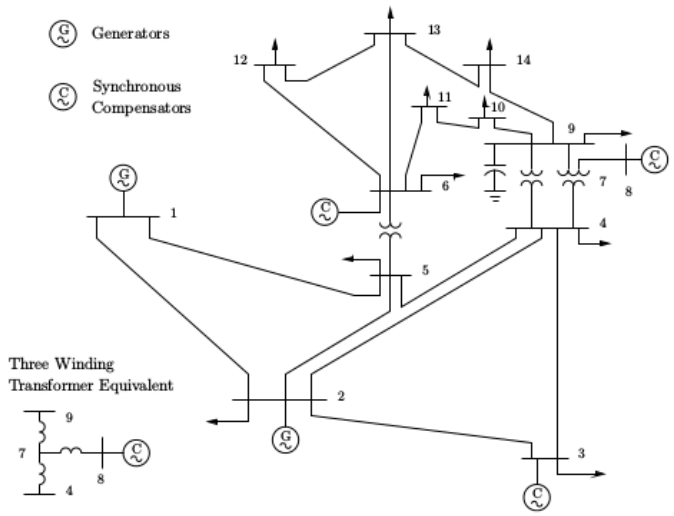

Fig. 8. Single-line diagram of the IEEE 14-bus system.

this section is described by the following DAEs:

$$
\begin{aligned}
T_w\dot{v}_1 &= -K_w v_{si} - v_1\,,\\
T_2\dot{v}_2 &= \Big(1-\frac{T_1}{T_2}\Big)(K_w v_{si}+v_1) - v_2\,,\\
T_4\dot{v}_3 &= \Big(1-\frac{T_3}{T_4}\Big)\Big(v_2+\frac{T_1}{T_2}(K_w v_{si}+v_1)\Big) - v_3\,,\\
0 &= v_3+\frac{T_3}{T_4}\Big(v_2+\frac{T_1}{T_2}(K_w v_{si}+v_1)\Big) - v_{so}\,,
\end{aligned}
$$

where v_1, v_2, v_3 are the PSS state variables; T_w, T_1, T_2, T_3, T_4 are time constants; K_w is the PSS gain. In addition, the input v_{si} is the local rotor speed, which, depending on the examined scenario, may be delayed or not. Finally, the output signal v_{so} is an additional input to the local AVR reference, so that the PSS provides damping of electromechanical oscillations through excitation control. The PSS block diagram is depicted in Fig. 9.

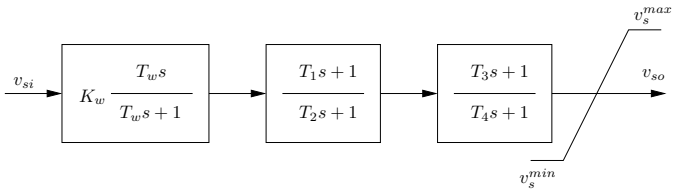

Fig. 9. Power system stabilizer block diagram.

To study the effect of time-delayed damping control on the small signal stability of the IEEE 14-bus system, two damping control configurations are compared, namely, a conventional PSS with delayed input signal; and a PSS that consists of two channels, one delayed and one non-delayed. In both cases, the damping controller is installed at the AVR of the synchronous machine connected at bus 1.

The impact of time delay in each case is evaluated by means of constructing the ζ-stability map in the delay-control gain space. For each point of the plane, an eigenvalue analysis is carried out by applying the Chebyshev discretization technique (see Section II-C). The spectrum of the approximate matrix pencil is calculated using the QR algorithm with LAPACK [44]. Then, comparison among the eigenvalues allows obtaining the most poorly damped one determining the ζ-stability.

A. Standard PSS with Delayed Input Signal

The employed PSS model is as shown in Fig. 9. The control input signal is considered to be the delayed local rotor speed measurement:

$$v_{si} = \omega_1(t-\tau)\ , \tag{39}$$

where τ is an intentional constant delay. The PSS time constant values are summarized in Table I.

TABLE I
IEEE 14-BUS SYSTEM: PSS PARAMETERS.

$T_1 = T_3 = 0.28$ s, $T_2 = T_4 = 0.02$ s, $T_w = 10$ s

The dynamic order of the system is 54. Setting the number of points of the Chebyshev differentiation matrix to $N_C = 10$ yields 540 eigenvalues in total. The system ζ-stability map in the τ-K_w plane is shown in Fig. 10. The map consists of distinct and not compact stable regions, which stems from the fact that, without the PSS, the system is unstable. For $K_w \in (-0.55, 0.65)$, the system is unstable regardless of the magnitude of the delay. The delay margin of the system is 0.104 s and is obtained for $K_w = 1.5$. Moreover, using the standard PSS with a negative gain value leads necessarily to instability. Finally, operation under the presence of a large delay, e.g. 0.35 s, is infeasible.

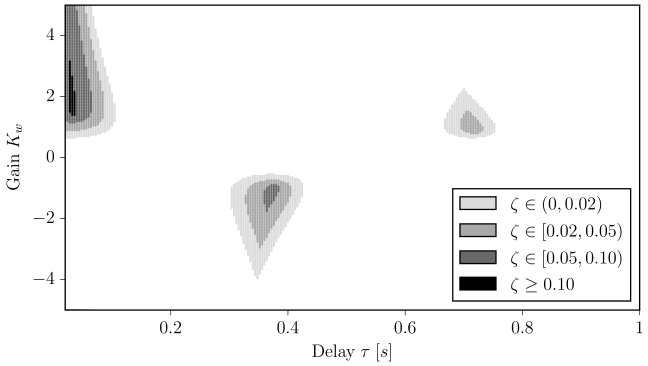

Fig. 10. IEEE 14-bus system: ζ-stability map in the τ-K_w plane ($\zeta_{\max} = 0.11$).

B. Dual-channel PSS

In the OMIB system example of Section III, a compact stable region in the delay-control gain plane can be achieved by employing a PR-based PSS scheme, tuned to operate the system at a point with good damping characteristics. The same principle can be applied to the IEEE 14-bus system. With this aim, a PSS with two control channels, one not delayed and one delayed, is examined. The scheme of the dual-channel PSS is shown in Fig. 11.

The Non-Retarded PSS (NRPSS) is tuned to render the non-delayed system small signal stable. The control input of

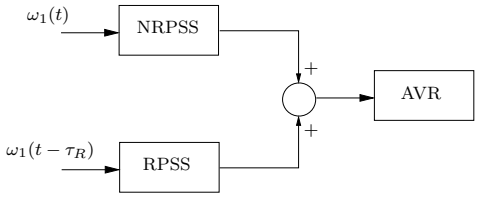

Fig. 11. Dual-channel PSS configuration.

NRPSS is the local rotor speed $\omega_1(t)$. The Retarded PSS (RPSS) tunes the delay dynamics so that the system operates at a point with good damping characteristics. The input signal of the RPSS is the delayed rotor speed $\omega_1(t-\tau_R)$, where $\tau_R \geq 0$ is the magnitude of the delay. The time constants of both NRPSS and RPSS are as summarized in Table I. In addition, $K_{w,P}$ and $K_{w,R}$ denote the gains of NRPSS and RPSS, respectively. An analogy between the dual-channel PSS configuration and the PR-based PSS of the OMIB system example of Section III is given in Table II.

TABLE II
ANALOGY BETWEEN THE EXAMINED DUAL-CHANNEL PSS CONFIGURATION AND THE PR CONTROL OF SECTION III.

System	OMIB	IEEE 14-bus
Non-retarded control	Proportional k_p	NRPSS
Retarded control	k_r, τ_r	RPSS

The NRPSS gain is tuned so that the system without delayed control is small signal stable. For $K_{w,P}=5$, $K_{w,R}=0$, SSSA shows that the rightmost pair of eigenvalues is $-0.1376 \pm j0.0203$. The most poorly damped pair is $-0.5171 \pm j7.2516$, which yields a damping ratio 0.071.

Figure 12 shows the ζ-stability map of the system in the $K_{w,R}$-τ_R plane assuming $K_{w,P}=5$. In this case, the dynamic order of the system is 57 and, using $N_C=10$, 570 eigenvalues are calculated in total to obtain each point of the map. The resulting map shows that the stable region is compact, while the area with $K_{w,R} \in (-2.4, 2.5)$ is delay independent stable. Figure 12 also shows that the maximum damping is $\zeta_{\max} = 0.178$ and is achieved for $\tau = 0.34$ s, i.e. a relatively large delay value.

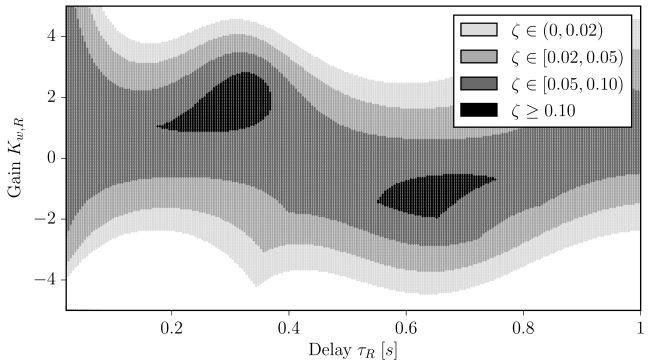

Fig. 12. IEEE 14-bus system: ζ-stability map in the τ_R-$K_{w,R}$ plane ($\zeta_{\max} = 0.178$).

C. Application to Wide Area Damping Control

The proposed approach has an interesting application to wide area measurement systems. A Wide Area Damping Controller (WADC) typically employs a signal that is remote, and thus has to be transmitted to the control actuator through a communication network, which introduces an inherent and unavoidable delay.

Considering that the delay fed to the dual-channel PSS (see Section IV-B) is inherent, the structure of Fig. 12 implies that if a proper artificial delay is injected on top of the inherent delay, the system can be led to a region of better damping characteristics[4]. This extra delay can be introduced, for example, by a properly designed controller that adjusts both the delay and gain values following a stable path, through consecutive quasi-steady state shifts of the system equilibrium.

The inherent delay can create a severe stability issue for the conventional PSS with delayed input signal (see Section IV-A and in particular Fig. 10), since the delay margin in this case is relatively small (0.104 s). For an inherent delay that has a small magnitude, a delay-dependent design of the standard PSS allows increasing the delay margin and may be adequate to avoid instability. In fact, in Fig. 10, the region of the highest damping $\zeta \geq 0.10$ is obtained for a non-zero delay value, with the maximum damping ratio value being $\zeta_{\max} = 0.11$. The closed-loop loci related to the critical system mode have an angle of departure closer to 180° when $\tau = 0.03$ s. In other words, the phase shift introduced by the PSS is optimal when a small delay is present.

Another technique commonly employed to mitigate destabilizing delay effects is time delay compensation. The main idea of delay compensation is to apply a control block which generates a signal that is similar to the original, non-delayed signal. The compensated signal is then fed to the PSS. Let consider an example using the classical Proportional-Derivative (PD) delay compensation method [45], [46]. With $K_w = 1.5$, the ζ-stability map in the delay vs delay compensation gain (τ-K_τ) is shown in Fig. 13. The inclusion of the PD compensation to a conventional PSS with delayed input signal increases the delay margin of the system to 0.184 s, while oscillations have a damping ratio $\zeta \geq 0.10$ but only for delays smaller than 0.121 s. That is, delay compensation cannot handle large communication delays. On the other hand, as already discussed, the dual-channel PSS can be adaptively tuned to achieve good damping characteristics for a wide range of communication delays.

So far, a constant delay model for the inherent communication delay has been considered. While WAMS delays are time-varying, assuming constant delays in power system damping control applications is conservative [38], [47]. Although the constant delay analysis provides valuable insights, for completeness, and in order to ensure that arbitrary deviations of delays do not compromise stability of the system, e.g., see [48], it is relevant to study also via time simulations the impact of the proposed approach on the transient response of the IEEE 14-bus system with inclusion of a stochastic delay model.

[4]Outside the power systems literature there is theoretical and experimental evidence of this 'delay scheduling' idea [9].

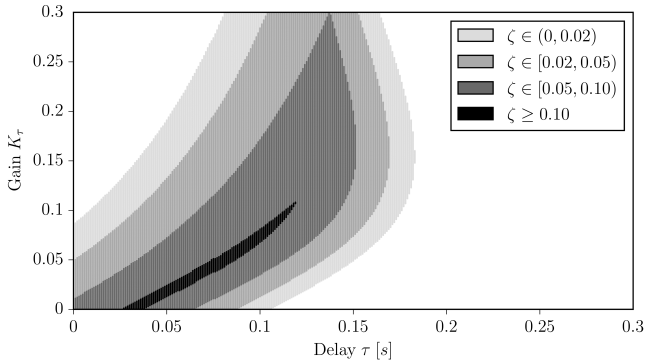

Fig. 13. IEEE 14-bus system with delay compensation: ζ-stability map ($\zeta_{\max} = 0.112$).

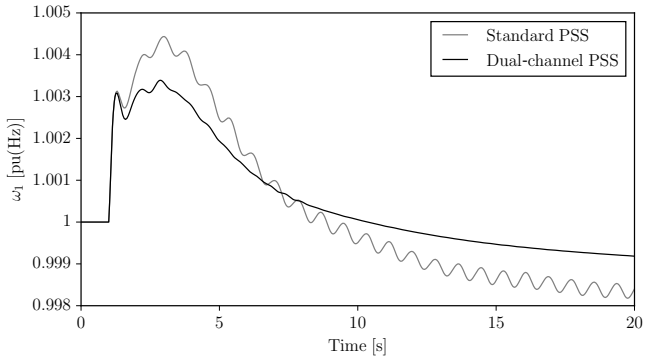

Fig. 15. IEEE 14-bus system with WAMS delay: Response following a three-phase fault.

To this aim, the realistic time-varying WAMS delay model proposed in [28] is employed. This model is as follows:

$$\tau(t) = \tau_c + \tau_p(t) + \tau_s(t) \ , \tag{40}$$

where τ_c is a constant component that expresses the processing time of the measurement unit plus the inevitable delay imposed by the communication medium; $\tau_p(t)$ is a periodic component arising from the fact that that data packets are sent repeatedly in discrete time instants; and $\tau_s(t)$ is a stochastic component modeling uncertainties and noises during the transmission, including the probability of a dropout. The profile of the WAMS delay $\tau(t)$ considered in this example, as well as the corresponding average constant delay $\bar{\tau}$, are shown in Fig. 14.

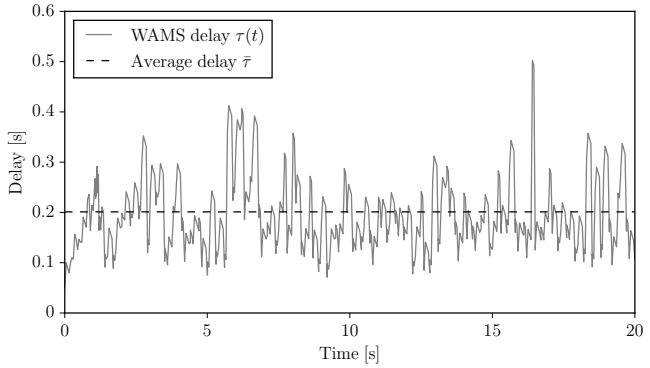

Fig. 14. WAMS delay (40) and average constant delay $\bar{\tau}$.

Two scenarios are compared: (i) system with inclusion of the standard PSS with delayed input and (ii) system with inclusion of the dual-channel PSS. The gain and artificial delay of the dual-channel PSS are tuned based on the stability map in Fig. 12. The system operates around the point $(0.62, -0.15)$, which corresponds to an equilibrium with $\zeta \geq 0.10$. The average delay of the WAMS delay is $\bar{\tau} = 0.201$ s, and thus the dual-channel PSS adds an extra constant delay equal to 0.419 s.

A three-phase fault is simulated at bus 3 of the IEEE-14 bus system. The fault occurs at $t = 1$ s and is cleared after 0.12 s by tripping the line that connects buses 2 and 3. The trajectory of the rotor speed of the synchronous machine connected at bus 1 is shown in Fig. 15. As expected, using the standard PSS leads to an unstable oscillation of increasing amplitude, since the considered WAMS delay is larger than the delay margin of the system (see Fig.10). On the other hand, the dual-channel PSS properly damps the electromechanical oscillation.

V. Conclusions

This paper presents new results on time-delayed damping control of power system synchronous machine electromechanical oscillations. The paper shows that injecting delays in a PSS can, under certain conditions, significantly improve the dynamic response of the overall system. The paper focuses on the delay-control gain space, and studies the stability boundaries, as well as the relationship between the existence of delay-independent stability and connected stability domains in the system parameters Connected stable regions are obtained by employing a PSS with two control channels and indicate that best damping characteristics may be achieved for larger delay values. Connectedness in this context enables the utilization of a large range of stabilizing parameters without the system having to jump over destabilizing settings. Future work will focus on the application of domain knowledge like the property of passivity, see, e.g. [49], to benchmark the performance of passivity-based controllers.

References

[1] H. Wu, H. Ni, and G. T. Heydt, "The impact of time delay on robust control design in power systems," in *Procs of the 2002 IEEE Power Eng. Society Winter Meeting*, 2002.

[2] J. W. Stahlhut, T. J. Browne, G. T. Heydt, and V. Vittal, "Latency viewed as a stochastic process and its impact on wide area power system control signals," *IEEE Trans. Power Syst.*, vol. 23, no. 1, pp. 84–91, Feb. 2008.

[3] F. Milano and M. Anghel, "Impact of time delays on power system stability," *IEEE Trans. Circ. Syst. - I: Regular Papers*, vol. 59, no. 4, pp. 889–900, Apr. 2012.

[4] R. Sipahi, S. I. Niculescu, C. T. Abdallah, W. Michiels, and K. Gu, "Stability and stabilization of systems with time delay," *IEEE Control Syst. Mag.*, vol. 31, no. 1, pp. 38–65, 2011.

[5] K. Pyragas, "Continuous control of chaos by self-controlling feedback," *Phys. Lett. A*, vol. 170, no. 6, pp. 421–428, 1992.

[6] R. Sipahi and N. Olgac, "Complete stability robustness of third-order LTI multiple time-delay systems," *Automatica*, vol. 41, no. 8, pp. 1413–1422, 2005.

[7] G. Stépán, *Retarded dynamical systems: stability and characteristic function*. New York, USA: Longman Scientific & Technical, 1989.

[8] C. T. Abdallah, P. Dorato, J. Benites-Read, and R. Byrne, "Delayed positive feedback can sabilize oscillatory systems," in *Proc. Amer. Control Conf.*, San Francisco, CA, USA, June 1993, pp. 3106–3107.

[9] N. Olgac, A. F. Ergenc, and R. Sipahi, "Delay scheduling: a new concept for stabilization in multiple delay systems," *J. Vibration Control*, vol. 11, no. 9, pp. 1159–1172, 2005.

[10] A. Ramírez, R. Garrido, and S. Mondié, "Velocity control of servo systems using an integral retarded algorithm," *ISA Trans.*, vol. 58, pp. 357–366, 2015.

[11] A. Ramírez, S. Mondié, R. Garrido, and R. Sipahi, "Design of proportional-integral-retarded (PIR) controllers for second-order LTI systems," *IEEE Trans. Autom. Control*, vol. 61, no. 6, pp. 1688–1693, Jun. 2016.

[12] A. Ramírez, R. Sipahi, S. Mondié, and R. Garrido, "An analytical approach to tuning of delay-based controllers for LTI-SISO systems," *SIAM J. Control Optim.*, vol. 55, no. 1, pp. 397–412, 2017.

[13] K. Abidi, Y. Yildiz, and B. E. Korpe, "Explicit time-delay compensation in teleoperation: An adaptive control approach," *Int. J. Robust Nonlinear Control*, vol. 26, no. 15, pp. 3388–3403, 2016.

[14] D. Helbing, S. Lämmer, T. Seidel, P. Šeba, and T. Płatkowski, "Physics, stability, and dynamics of supply networks," *Phys. Rev. E*, vol. 70, no. 6, 2004, art. no. 066116.

[15] G. Orosz, R. E. Wilson, and G. Stépán, "Traffic jams: dynamics and control," *Philos. Trans. Roy. Soc. London A, Math. Phys. Sci.*, vol. 368, no. 1928, pp. 4455–4479, 2010.

[16] R. Olfati-Saber, "Ultrafast consensus in small-world networks," in *Procs Amer. Control Conf.*, Portland, OR, USA, June 2005, pp. 2371–2378.

[17] W. Qiao and R. Sipahi, "Consensus control under communication delay in a three-robot system: Design and experiments," *IEEE Trans. Control Syst. Technol.*, vol. 24, no. 2, pp. 687–694, 2016.

[18] K. Gopalsamy, *Stability and Oscillations in Delay Differential Equations of Population Dynamics*. Norwell, MA: Kluwer, 1992.

[19] R. Bellman and K. L. Cooke, *Differential-Difference equations*. New York, USA: Academic Press, 1963.

[20] J. K. Hale and S. M. V. Lunel, *Introduction to functional differential equations*. New York, USA: Springer-Verlag, 1993.

[21] E. Fridman and L. Shaikhet, "Simple LMIs for stabilization by using delays," in *Proceedings of the IEEE Conference on Decision and Control*, 2016, pp. 3240–3245.

[22] H. Kokame, K. Hirata, K. Konishi, and T. Mori, "Difference feedback fan stabilize uncertain steady states," *IEEE Trans. Autom. Control*, vol. 46, no. 12, pp. 1908–1913, 2001.

[23] A. G. Ulsoy, "Time-delayed control of SISO systems for improved stability margins," *J. Dyn. Syst. Meas. Control*, vol. 137, no. 4, pp. 558–563, 2015.

[24] O. J. Smith, "A controller to overcome dead time," *ISA Journal*, vol. 6, no. 2, pp. 28–33, 1959.

[25] H. E. Kallman, "Transversal filters," *Proceedings of the IRE*, vol. 28, pp. 302–10, 1940.

[26] A. Ramírez and R. Sipahi, "Multiple intentional delays can facilitate fast consensus and noise reduction in a multiagent system," *IEEE Trans. Cybern.*, 2018, DOI: 10.1109/TCYB.2018.2798163.

[27] S. Wang, X. Meng, and T. Chen, "Wide-area control of power systems through delayed network communication," *IEEE Trans. Control Syst. Technology*, vol. 20, no. 2, pp. 495–503, Mar. 2012.

[28] M. Liu, I. Dassios, G. Tzounas, and F. Milano, "Stability analysis of power systems with inclusion of realistic-modeling WAMS delays," *IEEE Trans. Power Syst.*, vol. 34, no. 1, pp. 627–636, Jan. 2019.

[29] F. Milano, "Small-signal stability analysis of large power systems with inclusion of multiple delays," *IEEE Trans. Power Syst.*, vol. 31, no. 4, pp. 3257–3266, Jul. 2016.

[30] C. Li, Y. Chen, T. Ding, Z. Du, and F. Li, "A sparse and low-order implementation for discretization-based eigen-analysis of power systems with time-delays," *IEEE Trans. Power Syst.*, vol. 34, no. 6, pp. 5091–5094, Nov. 2019.

[31] R. Asghari, B. Mozafari, M. Salay Naderi, T. Amraee, V. Nurmanova, and M. Bagheri, "A novel method to design delay-scheduled controllers for damping inter-area oscillations," *IEEE Access*, vol. 6, pp. 71 932–71 946, 2018.

[32] S. Roy, A. Patel, and I. N. Kar, "Analysis and design of a wide-area damping controller for inter-area oscillation with artificially induced time delay," *IEEE Trans. Smart Grid*, vol. 10, no. 4, pp. 3654–3663, Jul. 2019.

[33] S. I. Niculescu, *Delay Effects on Stability: A Robust Control Approach*. Springer-Verlag, 2001.

[34] R. Datko, "A procedure for determination of the exponential stability of certain differential-difference equations," *Quart. Appl. Math.*, vol. 36, no. 3, pp. 279–292, 1978.

[35] A. Ramírez, "Design of maximum exponential decay rate for LTI-SISO systems via delay-based controllers," Ph.D. dissertation, CINVESTAV, México City, México, 2015.

[36] A. Bellen and S. Maset, "Numerical solution of constant coefficient linear delay differential equations as abstract cauchy problems," *Numerische Mathematik*, vol. 84, no. 3, pp. 351–374, Jan. 2000.

[37] D. Breda, S. Maset, and R. Vermiglio, *Stability of Linear Delay Differential Equations: A Numerical Approach with MATLAB*. New York, USA: Springer, 2015.

[38] G. Tzounas, M. Liu, M. A. A. Murad, and F. Milano, "Stability analysis of wide area damping controllers with multiple time delays," *IFAC-PapersOnLine*, vol. 51, no. 28, pp. 504 – 509, 2018, 10th IFAC Symposium on Control of Power and Energy Syst. CPES 2018.

[39] F. Milano and I. Dassios, "Small-signal stability analysis for non-index 1 Hessenberg form systems of delay differential-algebraic equations," *IEEE Trans. Circ. Syst. I: Regular Papers*, vol. 63, no. 9, pp. 1521–1530, Sep. 2016.

[40] P. Kundur, *Power System Stability and Control*. New York: Mc-Grall Hill, 1994.

[41] I. Kamwa, R. Grondin, and Y. Hebert, "Wide-area measurement based stabilizing control of large power systems-a decentralized/hierarchical approach," *IEEE Trans. Power Syst.*, vol. 16, no. 1, pp. 136–153, Feb. 2001.

[42] F. Milano, *Power System Modelling and Scripting*. London: Springer, 2010.

[43] ——, "A Python-based software tool for power system analysis," in *Procs of the IEEE PES General Meeting*, Jul. 2013.

[44] E. Angerson, Z. Bai, J. Dongarra, A. Greenbaum, A. McKenney, J. D. Croz, S. Hammarling, J. Demmel, C. Bischof, and D. Sorensen, "LAPACK: A portable linear algebra library for high-performance computers," in *Procs of the ACM/IEEE Conf. on Supercomputing*, Nov. 1990.

[45] Y.-C. Tian and D. Levy, "Compensation for control packet dropout in networked control systems," *Information Sciences*, vol. 178, no. 5, pp. 1263 – 1278, 2008.

[46] M. Liu, I. Dassios, G. Tzounas, and F. Milano, "Model-independent derivative control delay compensation methods for power systems," *Energies*, vol. 13, no. 2, p. 342, 2020.

[47] M. Liu, I. Dassios, and F. Milano, "Delay margin comparisons for power systems with constant and time-varying delays," *Electric Power Syst. Research*, vol. 190, p. 106627, 2021.

[48] D. Soudbakhsh, A. Chakrabortty, and A. M. Annaswamy, "A delay-aware cyber-physical architecture for wide-area control of power systems," *Control Eng. Practice*, vol. 60, pp. 171 – 182, 2017.

[49] N. Chopra, "Passivity results for interconnected systems with time delay," in *Procs of the IEEE Conference on Decision and Control*, 2008.

Georgios Tzounas (S'17) received from National Technical University of Athens, Greece, the ME in Electrical and Computer Engineering in 2017. Since September 2017, he is a Ph.D. candidate with University College Dublin, Ireland. His scholarship is funded through the SFI Investigator Award with title "Advanced Modelling for Power System Analysis and Simulation" (AMPSAS). His current research interests include stability analysis and robust control of power systems.

Rifat Sipahi (SM'16) received the B.Sc. degree in mechanical engineering from Istanbul Technical University, Istanbul, Turkey, in 2000, and the M.Sc. and Ph.D. degrees in mechanical engineering from the University of Connecticut, Storrs, CT, USA, in 2003 and 2005, respectively. He was a post-doctoral fellow with HeuDiaSyC (CNRS) Labs, Université de Technologie de Compiègne, Compiègne, France, from 2005 to 2006. In 2006, he joined the Department of Mechanical and Industrial Engineering, Northeastern University, Boston, MA, USA, where he is currently a Professor. His current research interests include stability, stabilization of dynamical systems at the interplay between multiple time delays and network graphs, human–machine systems, and human–robotic interactions. Sipahi is an Associate Editor of Automatica and a Fellow of ASME.

Federico Milano (F'16) received from the Univ. of Genoa, Italy, the ME and Ph.D. in Electrical Engineering in 1999 and 2003, respectively. From 2001 to 2002 he was with the University of Waterloo, Canada, as a Visiting Scholar. From 2003 to 2013, he was with the Universtiy of Castilla-La Mancha, Spain. In 2013, he joined the University College Dublin, Ireland, where he is currently Professor of Power Systems Control and Protections and Head of Electrical Engineering. He is an IEEE PES Distinguished Lecturer, an associate editor of the IEEE Transactions on Power Systems and an IET Fellow. He is the secretary of the IEEE Power System Stability Controls Subcommittee. His research interests include power system modelling, control and stability analysis.